

Improved Coverage and Connectivity via Weighted Node Deployment in Solar Insecticidal Lamp Internet of Things

Fan Yang, Lei Shu, *Senior Member, IEEE*, Yuli Yang, *Senior Member, IEEE*, Ye Liu, Timothy Gordon

Abstract—As an important physical control technology, Solar Insecticidal Lamp (SIL) can effectively prevent and control the occurrence of pests. The combination of SILs and Wireless Sensor Networks (WSNs) initiates a novel agricultural Internet of Things (IoT), i.e., SIL-IoTs, to simultaneously kill pests and transmit pest information. In this paper, we study the weighted SIL Deployment Problem (wSILDP) in SIL-IoTs, where weighted locations on ridges are prespecified and some of them are selected to deploy SILs. Different from the existing studies whose optimization objective is to minimise the deployment cost, we consider the deployment cost and the total weight of selected locations jointly. We formulate the wSILDP as the Weighted Set Cover (WSC) problem and propose a Layered Deployment Method based on Greedy Algorithm (LDMGA) to solve the defined optimization problem. The LDMGA is composed of two phases. Firstly, SILs are deployed layer by layer from the boundary to the centre until the entire farmland is completely covered. Secondly, on the basis of three design operations, i.e., substitution, deletion and fusion, the suboptimal locations obtained in the first phase are fine-tuned to achieve the minimum deployment cost together with the maximum total weight for meeting the coverage and connectivity requirements. Simulation results clearly demonstrate that the proposed method outperforms three peer algorithms in terms of deployment cost and total weight.

Index Terms—Solar insecticidal lamp internet of things (SIL-IoTs), weighted solar insecticidal lamp deployment problem (wSILDP), weighted set cover (WSC) problem, restricted deployment locations, approximation algorithm, wireless sensor network (WSN).

I. INTRODUCTION

In recent years, with the improvement of living standards, more and more people are concerned about the source of their

food. The major focus is on the quality and safety of agricultural products, which can be guaranteed by effectively controlling diseases and pests. As an important technology of physical prevention and control, Solar Insecticidal Lamps (SILs) have been widely used for pest control. Through combining SILs with Wireless Sensor Networks (WSNs), a novel agricultural Internet of Things (IoT), referred to as SIL-IoTs, is established to simultaneously kill pests and transmit pest information. As shown in Fig. 1, this new-type SIL can estimate the number of pests killed by itself, based on the statistics of discharge times [1]. Meanwhile, with the aid of WSNs, the pest information can be delivered to subscribers, e.g., farmers or plant protection personnel, via a single hop or multi-hop connections, for assisting them in making reasonable decisions on the schedule and quantity of chemical control [2].

One of the most critical issues in SIL-IoTs is the SIL node deployment, and its primary objective is to achieve the optimal coverage of SIL without violating the full connectivity requirement. Similar with the coverage of industrial IoT, the coverage of SIL-IoTs is classified into three categories: 1) target coverage, 2) area coverage, and 3) barrier coverage. For the target coverage, SIL nodes are usually deployed at the locations where pests occur frequently. For the area coverage, SIL nodes are always deployed to achieve full coverage of the entire farmland. For the barrier coverage, SIL nodes are often deployed for the detection of pests' migration across the barrier. Since full coverage is preferred by most practical applications, the majority of current studies focus on the area coverage [3]. A fundamental concern for the area coverage is how to minimise the number of SIL nodes while completely covering the entire Region of Interest (RoI) and forming a connected network.

In the past decade, lots of research efforts have been done to solve the problem of area coverage. A top-down survey on the coverage and connectivity in this problem has been presented in [3]–[7], and we refer the reader to these comprehensive papers for more detailed discussions, where the common algorithms can be classified as: 1) deterministic algorithm [8]–[13], 2) heuristic algorithm [14]–[20], and 3) approximation algorithm [21]–[30]. We mainly review the related methods for solving the problem of area coverage in these three classifications. For example, in [11], the layered deployment model has been proposed to solve the area coverage problem in the scenario with characteristics of full coverage and irregular RoI, where sensor nodes are deployed from the centre to the periphery. Conversely, the authors in [12] have

Manuscript received September 28, 2020; revised Nov 30, 2020; accepted XX XX, XX. This work was supported in part by the Research Start-Up Fund for Talent Introduction of Nanjing Agricultural University under grant number 77H0603, and in part by the National Natural Science Foundation of China under Grant 62072248 and Grant 61902188, and in part by the Science and Technology Innovation Project of Xuzhou in 2018 under Grant KC18004, and in part by China Postdoctoral Science Foundation under Grant 2020T130304 and Grant 2019M651865. Lei Shu is the corresponding author.

F. Yang is with the College of Engineering, Nanjing Agricultural University, Nanjing, 210031, China and with School of Mathematics and Statistics, Jiangsu Normal University, Xuzhou, 221116, China (email: yangfan@jsnu.edu.cn).

L. Shu is with NAU-Lincoln Joint Research Center of Intelligent Engineering, Nanjing Agricultural University, China, 210031 and with School of Engineering in College of Science, University of Lincoln, UK, LN3235, Engineering Hub, Brayford Pool, Lincoln, LN67TS, United Kingdom (e-mail: lei.shu@ieee.org).

Y. Yang and T. Gordon are with School of Engineering, University of Lincoln, Lincoln LN6 7TS, United Kingdom (e-mail: yyang@lincoln.ac.uk; tgordon@lincoln.ac.uk).

Y. Liu is with the School of Artificial Intelligence, Nanjing Agricultural University, Nanjing, 210031, China (email: yeliu@njau.edu.cn).

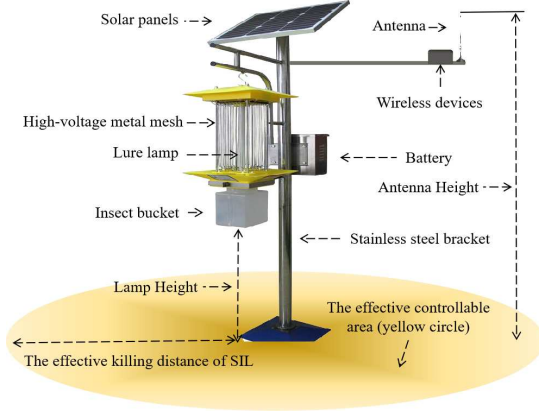


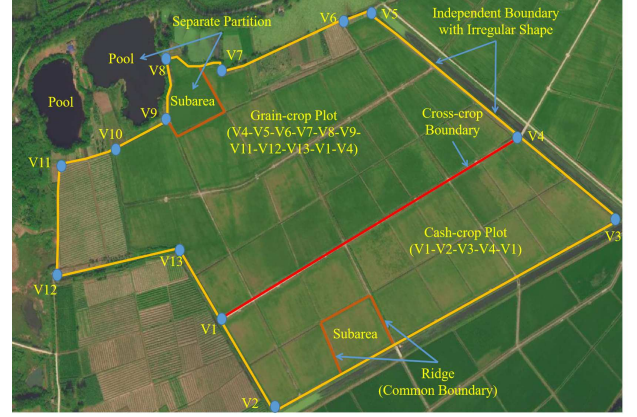
Fig. 1. An illustration of the new-type SIL node.

proposed the growth rings like deployment scheme, where sensor nodes are deployed from the boundary to the centre of the monitoring area. In [13], the projection-based approach has been presented for the area coverage in an arbitrary region with an irregular shape and inner obstacles. In [14], the authors have utilized Genetic Algorithm (GA) to minimize the deployment cost in actual farmland with irregular boundary and penetrable obstacles while meeting the full coverage and connectivity requirements. In [15], a nature-inspired GA has been proposed to maximize the network lifetime and coverage ratio while guaranteeing the minimum deployment cost. In [16], the authors have formulated the area coverage problem as the Mixed Integer Linear Program (MILP) problem, and proposed an iterative method based on GA to solve the defined optimization problem. Similarly, the node deployment problem has been formulated as the MILP problem in [21] as well, and the authors have developed the Direct-Search and Greedy-Search heuristic algorithms to minimise the number of deployed nodes while ensuring the energy neutral coverage and connectivity. The authors in [22] have presented a single phase multiple initiator algorithm, aiming to find the connect cover set for guaranteeing the coverage and connectivity. In [26], the authors have explored how to deploy the minimum number of nodes with local search algorithm and genetic algorithm while guaranteeing full coverage and connectivity.

Since the above previous works mainly focus on the 1-connectivity, we next review some related algorithms for k -connectivity ($k \geq 2$) [31]–[38]. In [33], the authors have presented a problem-specific constrained evolutionary algorithm to maximize the network coverage and lifetime objectives by effectively deploying sensor nodes and assign power while satisfying k -connectivity requirements. In [34], an efficient algorithm has been developed to address the fault-tolerant topology control problem in a heterogeneous wireless sensor network. In [35], the authors have proposed k -connectivity repair algorithms to minimize the number of additional nodes needed to repair the network connectivity. In [36], the authors have provided deployment patterns with proven optimality that achieve both coverage and k -connectivity in three dimensional networks. The authors in [37] have proposed a new deployment method using a GA to realize full coverage



(a)



(b)

Fig. 2. A farmland located in Babaiqiao Town, Nanjing, China ($118^{\circ}32'E$, $32^{\circ}11'N$): (a) overview, (b) the distribution of grain-crop plot and cash-crop plot.

and k -connectivity deployment for monitoring crop growth information of farmland on a large scale.

However, almost all existing works on the node deployment are based on the assumption that there is no constraint on the geographic location of nodes, i.e., the sensor nodes can be deployed anywhere, e.g., see [11]–[13]. Actually, this is too idealistic to be applied in practical agricultural applications. For instance, in an application of WSNs monitoring crop growth, there is a lower bound on the distance between sensor nodes and the farmland edge, to avoid the edge effect on the accuracy of monitoring information [37]. Moreover, most existing works also assume that the node deployment environment is homogeneous, i.e., the path loss is same for all locations, e.g., see [14]–[16]. In fact, the agricultural environment is non-static, where the propagation of radio waves are seriously affected by the reflection and refraction in the channels, the shadow fading due to the antenna setting, the height of crop canopy and the surrounding [39]. Additionally, most of existing efforts focus on minimizing the deployment cost without violating full coverage and connectivity requirements, e.g., [16], [26]. However, only minimising the deployment cost is far from the formulation of an actual agricultural application. For example, in a mixed-crop farmland, the cash crop has higher economic value than that of grain crop. Therefore, SIL nodes should be placed closer to the cash-crop regions while meeting the full coverage and connectivity requirements.



Fig. 3. An diagram of annual rings. The annual rings roll tightly and evenly from the outer to the inner of a stump until enveloping the cross section round by round, inspired by this, we propose the LDMGA, where SIL nodes are deployed layer by layer from the boundary to the centre until the entire farmland is completely covered.

Motivated by the above three issues, and on the basis of our previous work on the SIL Deployment Problem (SILDLP) [14], in this paper we study the weighted SILDLP (wSILDLP) in restricted locations, where the deployment of SIL nodes is restricted to a set of weighted locations on ridges. An actual farmland shown in Fig. 2 is studied in this paper, and the critical contributions of our study are summarized as follows:

- 1) To minimize the daily maintenance cost and reduce the impact on agricultural machinery services, SIL nodes are recommended to deploy on ridges. Therefore, we use a set of candidate locations on ridges to approximate the constraints on the locations of SILs and the constraints on the internode distance bound (from the perspective of either pest killing or internode communication). Meanwhile, to effectively model the actual agricultural applications, we assign a weight to each candidate location, and jointly optimise the deployment by maximising the total weight and minimising the deployment. Additionally, we formulate the wSILDLP in restricted locations as the Weight Set Cover (WSC) problem and prove that it is NP-hard. To the best of our knowledge, this work is the first to prove that the wSILDLP in restricted locations is NP-hard.
- 2) According to previous works on the analysis of propagation characteristics for wireless channels in various mono-crop plots, e.g., wheat [40], corn [41], rapeseed [42] and rice [43], we derive the maximum transmission distance between SIL nodes for a certain crop in maturity stage¹ based on the point-to-point communication model.
- 3) Inspired by the annual rings which roll tightly and evenly from the outer to the inner of a stump until enveloping the cross section round by round, as shown in Fig. 3, we propose a Layered Deployment Method based on Greedy Algorithm (LDMGA), where SIL nodes are deployed layer by layer from the boundary to the centre until the entire

¹The reason for choosing maturity stage as a representative of worst-case scenarios is that the plant stem and foliage are fully developed and the propagation environments are the worst. If a pair of SIL nodes can successfully communicate in maturity stage, they can certainly communicate during the whole growth cycle.

TABLE I
NOTATIONS

Notation	Description
m/n	Length / width of the network
ζ	Uniform length of grid
U / B	Set of PoIs / BPs
I_{EB} / I_{EA}	Effective boundary / arc intersection
W / w_l	Total weight / weight of l
ω	Weight coefficient
S	Set of SILs (Solution)
V	Boundary coverage vector (BCV)
G	Adjacency matrix of graph induced by S
L	Set of candidate locations
ρ	Candidate location density
R	Effective killing distance
R_c	Maximum transmission distance
P_i	Transmitted powers at SIL s_i
$\theta_{i,j}$	The channel coefficient between the transmitter s_i and the receiver s_j
$\phi_{i,j}$	Instantaneous received signal-to-noise ratio at SIL s_j with mean $\phi_{i,j}$
$n(t)$	A zero-mean additive white Gaussian noise with variance σ^2
γ_{th}	Predefined receiver sensitivity threshold
α	Path loss exponent
$P_{cov}^{A_f}(S, j)$	Coverage probability of PoI j in A_f
$C_{cov}^{A_f}(S)$	Coverage ratio of A
p_{size}	Size of initial population
$d(i, j)$	Euclidean distance between i and j
$ \cdot $	Number of cells in a set, i.e., cardinality
$\mathbb{E}(\cdot)$	Expectation operator

farmland is completely covered. Although the authors in [12] have used the same deployment strategy, they assume that there is no constraint on the geographic locations and the deployment environment is homogeneous, which cannot solve the wSILDLP in restricted locations. On the other hand, we design three operations, i.e., substitution, deletion and fusion, for the optimisation of the suboptimal solution obtained by LDMGA, to minimize the deployment cost and maximize the total weight while meeting the full coverage and connectivity requirements.

The rest of this paper is organized as follows. In Section II, we briefly introduce basic models. In Section III, we formulate the wSILDLP. Next, the proposed deployment method is described in detail in Section IV. We provide simulation results and discussions in Section V. Finally, we conclude this paper in Section VI.

II. PRELIMINARIES

A. Network Model

Given a rectangle network model whose length and width are m and n , respectively, there are $(m/\zeta) \times (n/\zeta)$ grid points, where ζ is the uniform length of each grid. Additionally, we assume that a farmland A is composed of two mono-crop plots: grain-crop plot A_G and cash-crop plot A_C . As show in Fig. 4, $A = \{A_f, A_{if}\}$, $A_f = \{A_f^1, A_f^2, \dots, A_f^{|A_f|}\}$, $A_{if} = \{A_{if}^1, A_{if}^2, \dots, A_{if}^{|A_{if}|}\}$, $A_C \cup A_G = A_f$ and $A_C \cap A_G = \emptyset$, where $|\cdot|$ denotes the number of cells in a set, i.e., cardinality. A_f^i represents the i^{th} feasible subarea, consisting of the ridge A_R^i and the planting region A_P^i . A_{if}^j represents the j^{th}

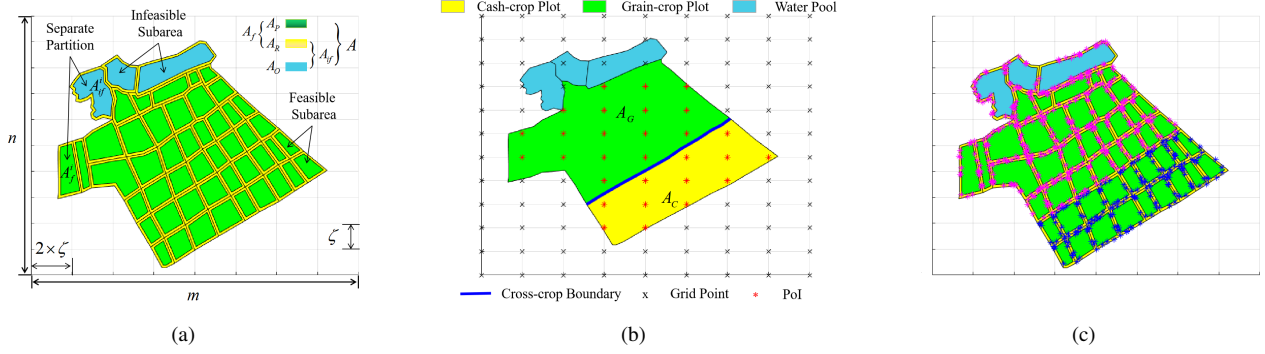


Fig. 4. Map 1: (a) the map used to model the actual farmland in Fig. 2, (b) the distribution of cash-crop plot A_C and grain-crop plot A_G , (c) a set of candidate locations L that are the only ones to deploy SIL nodes, where blue stars and pink stars represent the candidate locations in A_C and A_G , respectively.

infeasible subarea (e.g., water pool), consisting of the ridge A_R^j and the obstacle A_O^j . A_R is the area where SILs can be deployed, and A_P and A_O are the areas where SILs cannot be deployed, but wireless signals can pass through. Table I lists the notations used in this paper.

B. Definitions and Functions

Definition 1. Mono-crop plot is a homogeneous unit that can be characterised by the same channel propagation model. The transmission distance of candidate locations on ridges is the same in a mono-crop plot.

Definition 2. Cross-crop boundary is a common boundary between adjacent mono-crop plots.

Definition 3. Point of Interest (PoI) is a grid point in feasible subareas, i.e., the intended and monitored points. Let U be a set of PoIs.

Definition 4. Full coverage of A represents that all PoIs are covered by a set of SILs, denoted by $S = \{s_1, s_2, \dots, s_{|S|}\}$, where s_i is the i^{th} SIL node in S . Full connectivity of the network represents that any two SIL nodes in S can communicate with each other in the manner of a single hop or multi-hop.

Definition 5. Given a set of candidate locations L , as shown in Fig. 4(c), we define the weight of each element $l \in L$, denoted by w_l , as

$$w_l = \omega \frac{|C_C(l)|}{\pi R^2} + (1 - \omega) \frac{|C_G(l)|}{\pi R^2}, \quad (1)$$

where $\omega \in (0.5, 1)$ is the weight coefficient. $C_C(l)$ and $C_G(l)$ denote the PoI sets in A_C and A_G , respectively, within the effective killing distance R of the candidate location l . Fig. 5 shows an example of the weights for candidate locations in Fig. 4(c).

Definition 6. A SIL node s_i is a redundant one, if its effectively controllable area (see Fig. 1) is overlapped by other SIL nodes.

Definition 7. A PoI is defined as a Boundary Point (BP), if one of its one-hop neighbour grid points is not in A . Let B be a set of BPs.

TABLE II
FUNCTIONS

Function	Description
$C_C(l)$	Return the set of PoIs in A_C within the effective killing distance R of candidate location l
$C_G(l)$	Return the set of PoIs in A_G within the effective killing distance R of candidate location l
$X(l)$	Return the set of PoIs within the effective killing distance of candidate location l
$Y(p)$	Return the set of candidate locations that are able to cover point p
$Z(l)$	Return the set of candidate locations that can communicate with candidate location l
$H(l)$	Return the set of effective arc intersections within the effective killing distance of candidate location l
$W(S)$	Return the BCV V that is calculated by S
$J(V)$	Return the set of JPs in V

Definition 8. Given a solution S and a $[0,1]$ row vector whose dimension is $|B|$, its m^{th} element is 1 only if the m^{th} BP in B can be covered by any SIL node in S . Otherwise, this element is 0. This row vector is defined as the Boundary Coverage Vector (BCV). Let V be the BCV.

Definition 9. Given a BCV V , if the values of adjacent elements (the first and last elements are also considered as the adjacent elements) in V are different, Jump Point (JP) is the index of these two elements whose value is 0.

Definition 10. If the index of a BP in B is equal to JP, this BP is defined as a Boundary Intersection (BI). If a BI cannot be covered by any SIL node in S , it is an Effective Boundary Intersection (EBI). Arc Intersection (AI) is an intersection of two sensing circles². If an AI is within the farmland and the distance between this AI and any deployed SIL node $s \in S$ is not less than the effective killing distance of SIL s , this AI is defined as an Effective Arc Intersection (EAI). Let I_A be a set of AIs, I_{EA} be a set of EAIs, and I_{EB} be a set of EBIs.

Definition 11. The minimum bounding rectangle (MBR) is an expression of the polygon to the maximum extent representing

²For convenience, sensing circle is used to represent an SIL's effectively controllable area. The radius of sensing circle is equal to the effective killing distance.

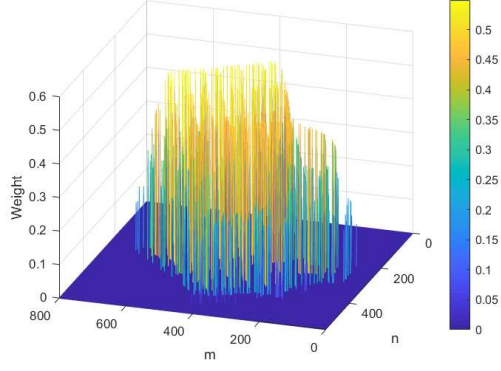


Fig. 5. An example of the weights for candidate locations in Fig. 4(c) with $m = 800$ metres, $n = 550$ metres, $\zeta = 1$ metre, $\omega = 0.55$ and $R = 60$ metres.

the shape of an actual farmland within the (x, y) coordinate system.

Let $X(l)$ denote the set of PoIs within the effective killing distance of candidate location l . Conversely, $Y(p)$ denotes the set of candidate locations that are able to cover the point p , and $Z(l)$ denotes the set of candidate locations that can communicate with the candidate location l . $H(l)$ represents the set of EAI within the effective killing distance of the candidate location l . $W(S)$ denotes the BCV V that is calculated by S , i.e., $V = W(S)$. $J(V)$ represents the set of JPs in V . These functions are listed in Table II.

For example, in Fig. 6, $S = \{l_1, l_2\}$, $U = \{1, 2, \dots, 15, 16\}$, $B = \{1, 2, \dots, 11, 12\}$ where $U(1) = B(1) = (3\zeta, 3\zeta)$, $|U| = 16$ and $|B| = 12$. The PoIs that can be covered by l_1 are $X(l_1) = \{4, 5, 14\}$. The candidate locations that can cover Point 17 are $Y(17) = \{l_1, l_2\}$. The candidate location that can communicate with l_2 is $Z(l_2) = \{l_1\}$. Since the EAI $I_{EA} = \{17\}$, we have $H(l_1) = H(l_2) = \{17\}$, $W(S) = \{0, 0, 0, 1, 1, 1, 0, 0, 0, 0, 0, 0\}$, and $J(V) = \{3, 7\}$, where $V = W(S)$ and $I_{EB} = \{3, 7\}$. Recall that $C_C(l)$ and $C_G(l)$ are the PoI sets in A_C and A_G within the effective killing distance R of candidate location l , respectively, we have $C_C(l_2) = \{15\}$, $C_G(l_2) = \{5, 6\}$, and $w_{l_2} = \omega/(\pi R^2) + 2(1 - \omega)/(\pi R^2) = (2 - \omega)/(\pi R^2)$.

C. Effective Killing Distance

In our previous survey paper [2], we have found that due to the difference of phototaxis, various kinds of pests have different requirements on the effective killing distance [44]–[47]. For example, the distance is about 24 metres for the tea leafhopper *Empoasca onukii* [45], but about 67 metres for the *Spodoptera litura Fabricius* [46].

Therefore, in this paper, we assume that for a certain kind of pest, the SIL node has a fixed effective killing distance. Moreover, we also assume that any Point j within the effective killing distance of SIL s_i can be directly covered by this SIL. Thus, the probability that Point j in A_f is covered by SIL s_i

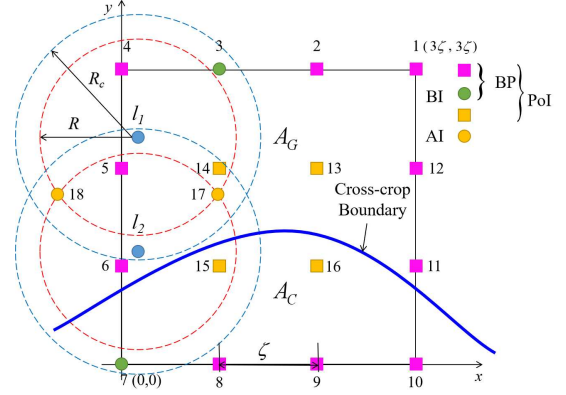


Fig. 6. An instance of deployment map with $U = \{1, 2, \dots, 15, 16\}$ and $B = \{1, 2, \dots, 11, 12\}$, i.e., $|U| = 16$ and $|B| = 12$. The blue dot represents the candidate location. The red dash circle represents the effective killing distance. The blue dash circle represents the maximum transmission distance.

can be derived as

$$f(s_i, j) = \begin{cases} 1, & d(s_i, j) \leq R \\ 0, & \text{otherwise} \end{cases} \quad (2)$$

where the operation $d(\cdot)$ is used to calculate the Euclidean distance between s_i and j .

It is worth noting that although there are multiple kinds of pests in actual farmland, we are concerned about one of the most common pests in crops. In other words, each candidate location in L has the same effective killing distance.

D. Maximum Transmission Distance

Since agricultural environment is non-static, the propagation of radio waves varies with the surrounding environment, e.g., canopy height [43] and plant density [48]. Therefore, to derive the maximum transmission distance of SIL nodes in actual farmland, the point-to-point communication model is used in this section.

Let s_i and s_j be the transmitter SIL node and receiver SIL node. The received signal at s_j can be expressed as [49]

$$r_j(t) = \sqrt{P_i} \theta_{i,j} s_i(t) + n(t) \quad (3)$$

where P_i is the transmitted power at node s_i , $\theta_{i,j}$ is the channel coefficient between s_i and s_j , $s_i(t)$ is the symbol transmitted by s_i at time t , and $n(t)$ is the AWGN with zero mean and variance σ^2 . The value of σ^2 is generally normalized to 1 [50].

Let $\phi_{i,j}$ and $\bar{\phi}_{i,j}$ be the instantaneous received signal-to-noise ratio (SNR) and the average received SNR at s_j , which can be expressed as [50]

$$\phi_{i,j} = \frac{P_i \theta_{i,j}^2}{\sigma^2} \quad (4)$$

and

$$\bar{\phi}_{i,j} = \frac{P_i \mathbb{E}(\theta_{i,j}^2)}{\sigma^2}, \quad (5)$$

respectively, where $\mathbb{E}(\theta_{i,j}^2)$ represents the variance of the channel coefficient. According to the distance-dependent path

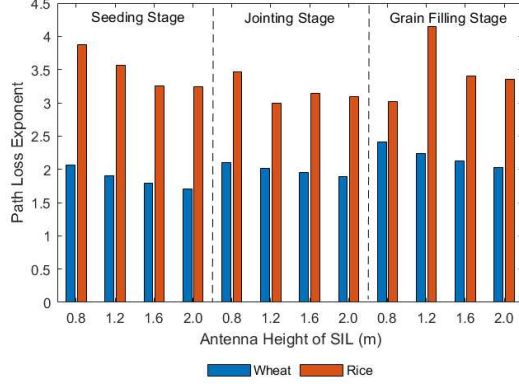


Fig. 7. An diagram of the relationship between growth stage and α for wheat [40] and rice [43].

loss model, the variance of the channel coefficient can be expressed as [51]

$$\mathbb{E}(\theta_{i,j}^2) = \left(\frac{d_0}{d(s_i, s_j)}\right)^\alpha, \quad (6)$$

where d_0 is the reference distance, usually set to 1 [51], and α is path loss exponent. Therefore, (5) can be rewritten as

$$\bar{\phi}_{i,j} = \frac{P_i}{\sigma^2} \left(\frac{d_0}{d(s_i, s_j)}\right)^\alpha. \quad (7)$$

According to previous works on the analysis of signal transmission characteristics in agricultural environment [40]–[43], [48], [52], [53], the path loss exponent α is different not only for different crops, but also for different growth stages for the same crop, as shown in Fig. 7. Since α is regarded as a good indicator for the communication possibility in agricultural environment, it is used to calculate the maximum transmission distance of SIL nodes. Therefore, we use α^l as the path loss exponent at candidate location l , and assume that the path loss exponent is the same for the candidate locations in the same mono-crop plot.

Let $R_c^{s_i}$ be the maximum transmission distance for SIL s_i according to α^{s_i} . A set of nodes that can successfully receive the information sent from s_i is restricted to the candidate locations that are within a distance $R_c^{s_i}$ from s_i . The following lemma shows how to determine the value of $R_c^{s_i}$.

Lemma 1. *For a SIL node s_j , it can successfully receive the information sent from s_i in an actual agricultural environment only if*

$$d(s_i, s_j) \leq R_c^{s_i} = d_0 \sqrt[\alpha^{s_i}]{\frac{P_i}{\sigma^2 \gamma_{th}}}, \quad (8)$$

where γ_{th} is a predetermined receiver sensitivity threshold.

Proof. As is known, s_j can successfully receive the information sent from s_i only if the average received SNR at s_j exceeds the receiver sensitivity threshold γ_{th} , i.e., $\bar{\phi}_{i,j} \geq \gamma_{th}$. Therefore, (7) can be expressed as

$$\frac{P_i}{\sigma^2} \left(\frac{d_0}{d(s_i, s_j)}\right)^{\alpha^{s_i}} \geq \gamma_{th}. \quad (9)$$

Thus, we have

$$d(s_i, s_j) \leq d_0 \sqrt[\alpha^{s_i}]{\frac{P_i}{\sigma^2 \gamma_{th}}} \quad (10)$$

Since $R_c^{s_i}$ is the maximum transmission distance of s_i , within which s_j can successfully receive the information sent from s_i , $R_c^{s_i}$ can be expressed as

$$R_c^{s_i} = d_0 \sqrt[\alpha^{s_i}]{\frac{P_i}{\sigma^2 \gamma_{th}}}. \quad (11)$$

□

However, it should be mentioned that due to the existence of asymmetric link between s_i and s_j caused by α^{s_i} and α^{s_j} , these two SIL nodes can communicate with each other only if $d(s_i, s_j) \leq \min(R_c^{s_i}, R_c^{s_j})$.

E. Metrics of SIL Deployment

In this paper, the following three metrics are considered.

1) Total weight

The total weight generated by S is denoted by W and expressed as

$$W = \sum_{i \in S} w_i. \quad (12)$$

2) Coverage

The probability of PoI k covered by any SIL node in S is denoted by $P_{cov}^{A_f}(S, k)$ and expressed as

$$P_{cov}^{A_f}(S, k) = 1 - \prod_{j=1}^{|S|} (1 - f(s_j, k)). \quad (13)$$

Therefore, the coverage ratio of A can be calculated as

$$C_{cov}^{A_f}(S) = \frac{\sum_{k=1}^{|U|} X_k}{|U|}, \quad (14)$$

where

$$X_k = \begin{cases} 1, & P_{cov}^{A_f}(S, k) = 1 \\ 0, & \text{otherwise} \end{cases} \quad (15)$$

3) Connectivity

Similar with that in [54], the following theorem of graph theory is used to check the network connectivity in this paper.

Theorem 1. *Let G be the adjacency matrix of graph induced by S and $M = [m_{ij}]_{i,j=1,2,\dots,|S|}$ be the matrix, where $M = G + G^2 + \dots + G^{|S|-1}$. Then, the graph is connected if and only if*

$$\forall i, j \in [1, |S|], m_{ij} \neq 0. \quad (16)$$

III. PROBLEM STATEMENT

With the aforementioned models, we describe and mathematically formulate our problem in this section. We also prove that this problem is NP-hard.

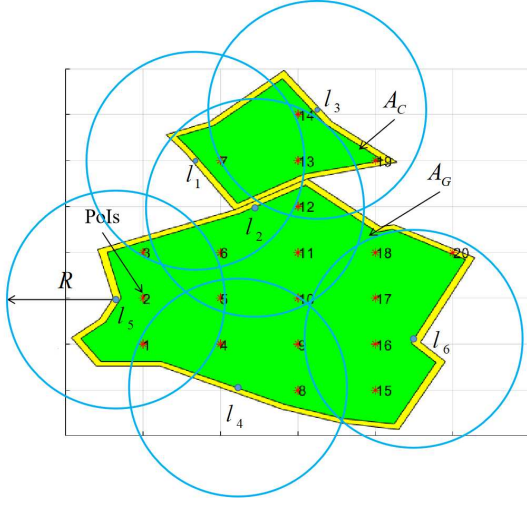


Fig. 8. An instance of $P1$: $U = \{1, 2, \dots, 20\}$ and $|U| = 20$, $L = \{l_1, l_2, \dots, l_6\}$ and $|L| = 6$. $l_1 = \{3, 6, 7, 13\}$, $l_2 = \{5, 6, 7, 10, 11, 12, 13, 14\}$, $l_3 = \{7, 12, 13, 14, 19\}$, $l_4 = \{1, 4, 5, 8, 9, 10\}$, $l_5 = \{1, 2, 3, 5\}$, $l_6 = \{15, 16, 17, 18, 20\}$. $w_1 = \frac{2}{\pi R^2}$, $w_2 = \frac{5-2\omega}{\pi R^2}$, $w_3 = \frac{1+3\omega}{\pi R^2}$, $w_4 = \frac{6-6\omega}{\pi R^2}$, $w_5 = \frac{4-4\omega}{\pi R^2}$, $w_6 = \frac{5-5\omega}{\pi R^2}$. Herein, $P1$ is to find a subset S of L such that the total weight is maximised, the size of S , i.e., $|S|$, is minimised, the graph induced by S is connected, and the union of S is U .

A. Problem Formulation

Given a set of weighted candidate locations L , our goal is to find a set of candidate locations S which can completely cover the entire farmland and form a connected network for maximising the total weight and minimising the set size, i.e., achieving the minimum deployment cost. This problem is denoted by $P1$, and the objective functions are formulated as

$$\max \sum_{i \in S} w_i \quad (17)$$

$$\min |S| \quad (18)$$

s.t.

$$\forall i \in [1, |S|], s_i \in L, |L| = \rho \times \sum_{j=1}^{|A|} A_A^j \quad (19)$$

$$C_{cov}^{A_f}(S) = 1 \quad (20)$$

$$\begin{aligned} \forall u, v \in [1, |S|], g_{uv} \in G, m_{uv} \in M, s \in S \\ g_{uv} = \begin{cases} 1, & d(s_u, s_v) \leq \min(R_c^u, R_c^v) \\ 0, & \text{otherwise} \end{cases} \quad (21) \\ M = G + G^2 + \dots + G^{|S|-1} \\ m_{uv} \neq 0 \end{aligned}$$

where (19) means that only candidate locations can be used to deploy SIL nodes, and (20) means that the solution S should meet the full coverage requirement. Additionally, (21) means that the graph induced by S , i.e., the network, is connected.

B. NP-Hardness Analysis

Theorem 2. The problem $P1$ is NP-hard.

Proof. The Weighted Set Cover (WSC) problem is one of the classical combinatorial optimization problems, which has been proved to be NP-hard. Given a universal set $U = \{1, 2, \dots, n\}$, a family $F = \{F_1, F_2, \dots, F_m\}$ of m subsets of U , a cost function (or weight function) associated with the family F , $C : F \rightarrow \mathbb{R}^+$, the problem is to find a set cover $F' \subseteq F$ such that the cost is minimum and the union of C is U , where $C(F_j)$ denotes the cost of the subset F_j .

For $P1$, a set of PoIs in A corresponds to U , and a collection of candidate locations $L = \{l_1, l_2, \dots, l_{|L|}\}$ corresponds to F . Each candidate location l_i is a subset of U and the weight function (1) corresponds to C . $P1$ is to find a subset S of L such that all PoIs in A are covered with the maximum total weight and the minimum size of S , i.e., $|S|$, while the graph induced by S is connected.

Therefore, $P1$ can be regarded as a WSC problem with additional constraints on collection size and network connectivity, i.e., $P1$ is a special case of the WSC problem. Since the WSC problem is NP-hard, $P1$ is NP-hard. An instance is given in Fig. 8. □

IV. THE PROPOSED NODE DEPLOYMENT SOLUTION

In this section, we propose a SIL node deployment method, i.e., LDMGA, to find the optimal solution for the wSILDP in restricted locations. LDMGA is a two-phase method. In the first phase, SIL nodes are deployed layer by layer from the boundary to the centre until the entire farmland is completely covered with a connected network, thus leading to a suboptimal solution. In the second phase, with the aid of three design operations, i.e., substitution, deletion and fusion, the suboptimal solution is fine-tuned towards the optimal locations to meet the full coverage and connectivity requirements, while achieving the maximum total weight and the minimum deployment cost. For clarity, the flowchart of LDMGA is shown in Fig. 9.

A. Layered Deployment Strategy

The layers in our LDMGA are classified into two categories: the first layer and the remaining layers except the first layer. The former is defined as the entire farmland, i.e., the bounded area formed by the vertices of a polygon shaping the actual farmland. The latter is defined as the sub-bounded area formed by a set of EAIs generated by S . An example in Fig. 10 illustrates these definitions.

In detail, to begin with, our LDMGA finds a suboptimal set of SIL nodes which can completely cover the boundary of the first layer with the maximum coverage ratio. Then, by iteratively covering the vertices of the new layer formed by EAIs, the optimal solution satisfying the requirements of full coverage and connectivity is obtained.

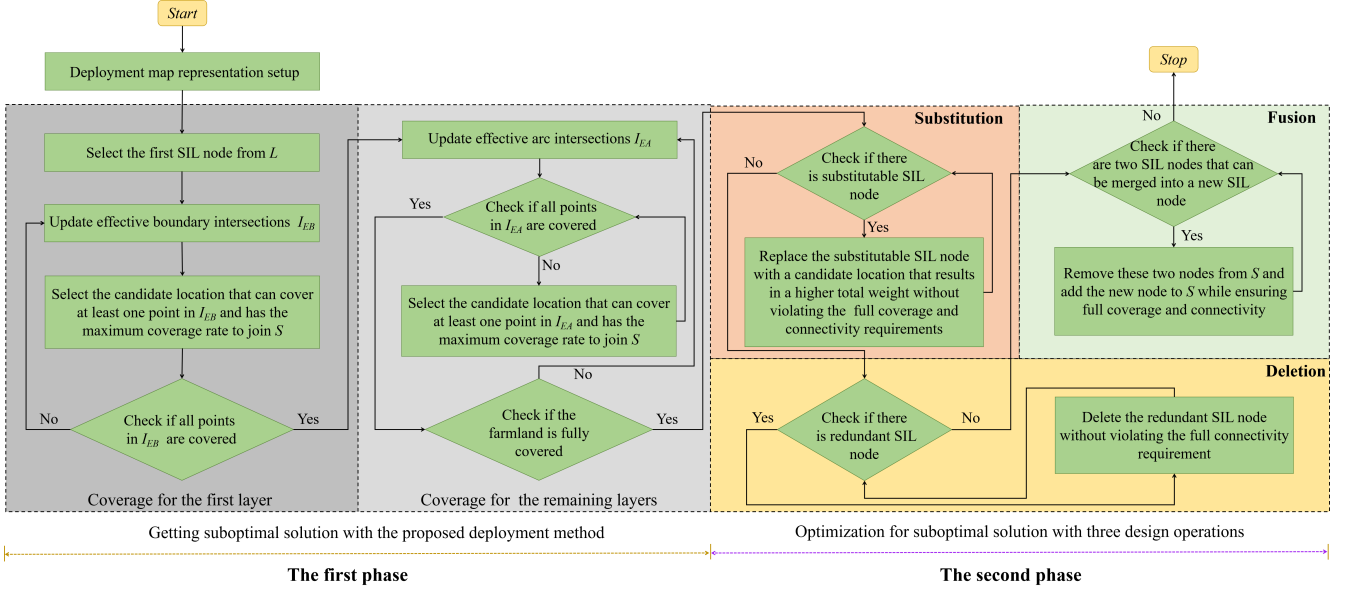


Fig. 9. Flowchart of our proposed deployment method LDMGA.

B. Deployment Map Representation Setup

Since the farmland is a continuous field, we need to discretize it into grid points based on ζ , which facilitates the calculation of coverage. On the basis of these grid points, a set of PoIs U and BPs B are determined, as shown in Fig. 4(b). Then, the area of each separate partition is calculated and sufficient candidate locations L are generated. Here, “sufficient” means that each PoI is covered by at least a candidate location and there is at least one route between two adjacent separate partitions with common boundary. Finally, the maximum transmission distance of each candidate location is determined according to (11).

C. Coverage for the First Layer

The purpose of our LDMGA’s first phase is to completely cover the boundary of the first layer, which consists of three steps: 1) selecting the first SIL node, 2) updating the EBIs I_{EB} , and 3) finding a set of SIL nodes that can completely cover the boundary of the first layer with the maximum coverage ratio. The pseudocode of coverage for the first layer is described in Algorithm 1.

1) *Selection of the first SIL node*: A candidate location l can be selected to deploy the first SIL node only if

$$l = \arg \max_{l^* \in L'} C_{Cov}^{Af}(l^*) \quad (22)$$

s.t.

$$L' = \bigcup_{i \in CP} Y(i), \quad (23)$$

where CP is a subset of the first layer’s vertices and each point in CP is on the MBR’s boundary. For example, $CP = \{V_1, V_2, V_3, V_5\}$ in Fig. 10. (22) means that candidate location in L' with the maximum coverage ratio is selected to deploy the first SIL node, and (23) means that at least one point in CP is covered by the first SIL node.

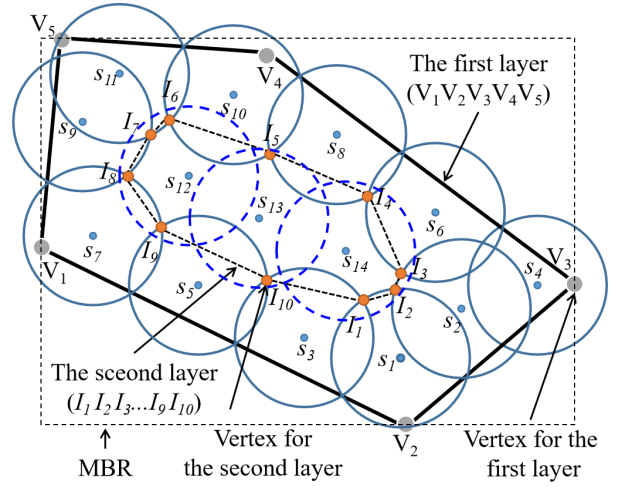


Fig. 10. An example illustrating the two kinds of layers in our LDMGA. Gray dots indicate the vertices of the polygon shaping the farmland, orange dots indicate the EAIs, and blue dots indicate deployed SIL nodes. The first layer is the bounded area formed by the vertices of a polygon shaping the farmland, i.e., $V_1 V_2 V_3 V_4 V_5$, and the second layer is the sub-bounded area, i.e., $I_1 I_2 \dots I_{10}$, formed by a set of EAIs generated by $\{s_1, s_2, \dots, s_{11}\}$. $S = \{s_1, s_2, \dots, s_{14}\}$, in which $\{s_1, s_2, \dots, s_{11}\}$ is used to cover the boundary of the first layer, and $\{s_{12}, s_{13}, s_{14}\}$ is used to cover the vertices of the second layer, i.e., the EAIs I_1 to I_{10} .

2) *Update of I_{EB}* : After adding a new candidate location to S , a set of EBIs, i.e., I_{EB} , needs to be updated. Recall that $J(V)$ returns a set of JPs in $V = W(S)$. Thus, $I_{EB} = B(J(V))$, i.e., Line 6 in Algorithm 1.

3) *Selection of the other SIL Nodes*: In addition to the first SIL node, candidate location l selected to cover the boundary of the first layer in each iteration should satisfy

$$l = \arg \max_{l^* \in (L'' \cap L''')} C_{Cov}^{Af}(l^*) \quad (24)$$

Algorithm 1 Coverage for the First Layer**Input:** CP, B, U **Output:** S

- 1: $S \leftarrow \emptyset$;
- 2: Identify the set of candidate locations L' that can cover any point in CP , i.e., $L' = \bigcup_{i \in CP} Y(i)$;
- 3: Select the candidate location l that has the maximum coverage ratio from L' , i.e., $l = \arg \max_{l^* \in L'} C_{Cov}^{A_f}(l^*)$;
- 4: Update solution, i.e., $S = S \cup l$;
- 5: **while** $C_{Cov}^B(S) \neq 1$ **do**
- 6: Update EBIs, i.e., $I_{EB} = B(J(W(S)))$;
- 7: Identify the set of candidate locations L'' that can cover any point in I_{EB} , i.e., $L'' = \bigcup_{i \in I_{EB}} Y(i) \setminus S$;
- 8: Identify the set of candidate locations L''' that can communicate with any SIL node in S , i.e., $L''' = \bigcup_{s \in S} Z(s) \setminus S$;
- 9: Select the candidate location l that has the maximum coverage ratio from $L'' \cap L'''$, i.e., $l = \arg \max_{l^* \in (L'' \cap L''')} C_{Cov}^{A_f}(l^*)$;
- 10: Update solution S , i.e., $S = S \cup l$;
- 11: **end while**
- 12: **Return** S ;

s.t.

$$L'' = \bigcup_{i \in I_{EB}} Y(i) \setminus S \quad (25)$$

$$L''' = \bigcup_{s \in S} Z(s) \setminus S \quad (26)$$

(24) means that among all candidate locations in $L'' \cap L'''$, l has the maximum coverage ratio. (25) means that at least one point in I_{EB} is covered by l . (26) means that the network built by $S \cup l$ is connected. An instance is given in Fig. 11(a).

D. Coverage for the Remaining Layers

Since all remaining layers is a sub-bounded area whose vertices are a set of EAs generated by S , the purpose of our LDMGA's second phase is to cover all vertices of these layers. The second phase consists of three steps: 1) updating EAs I_{EA} based on S , i.e., forming a new layer, 2) finding a set of SIL nodes that can cover all vertices of the remaining layers with the maximum coverage ratio, 3) repeating Steps 1) and 2) until the entire farmland is completely covered. The pseudocode of coverage for the remaining layers is described in Algorithm 2.

1) *Update of I_{EA}* : After completely covering all vertices of the remaining layers, we need to update I_{EA} for forming a new layer, where each point in I_{EA} , i.e., each vertex of the new layer, should satisfy

$$\forall i \in I_{EA}, \forall s \in S, d(i, s) \geq R, \quad (27)$$

i.e., See Line 2-15 in Algorithm 2.

Algorithm 2 Coverage for the Remaining Layers**Input:** S, R **Output:** S

- 1: **while** *true* **do**
- 2: $I_{EA} \leftarrow \emptyset$; $I_A \leftarrow \emptyset$;
- 3: **for** $m, n \in S, m \neq n$ **do**
- 4: **if** $d(m, n) \leq 2R$ **then**
- 5: Calculate arc intersections a between sensing circles of m and n ;
- 6: $I_A = I_A \cup a$;
- 7: **end if**
- 8: **end for**
- 9: **for** $i \in I_A$ **do**
- 10: **if** i is within the polygon shaping the actual farmland **then**
- 11: **if** $\forall s \in S, d(i, s) \geq R$ **then**
- 12: $I_{EA} = I_{EA} \cup i$;
- 13: **end if**
- 14: **end if**
- 15: **end for**
- 16: **if** $|I_{EA}| == 0$ **then**
- 17: **Stop**;
- 18: **else**
- 19: **while** $|I_{EA}| \neq 0$ **do**
- 20: Identify the set of candidate locations L'' that can cover any point in I_{EA} , i.e., $L'' = \bigcup_{i \in I_{EA}} Y(i) \setminus S$;
- 21: Identify the set of candidate locations L''' that can communicate with any SIL node in S , i.e., $L''' = \bigcup_{s \in S} Z(s) \setminus S$;
- 22: Select the candidate location l that has the maximum coverage ratio from $L'' \cap L'''$, i.e., $l = \arg \max_{l^* \in (L'' \cap L''')} C_{Cov}^{A_f}(l^*)$;
- 23: Update solution S , i.e., $S = S \cup l$;
- 24: $I_{EA} = I_{EA} \setminus (H(l) \cap I_{EA})$;
- 25: **end while**
- 26: **end if**
- 27: **end while**
- 28: **Return** S ;

2) *Selection of SIL Nodes*: A candidate location l can be selected to join S only if (24), (26) and (28) are satisfied, i.e.,

$$L'' = \bigcup_{i \in I_{EA}} Y(i) \setminus S \quad (28)$$

as shown in Line 20-23 in Algorithm 2.

It is worth noting that if the updated I_{EA} is empty, the second phase will be stopped since the entire farmland has been completely covered. Otherwise, the second phase will be performed until $I_{EA} = \emptyset$, i.e., see Line 16-26. An instance is given in Fig. 11(b).

E. Optimization of Solution

In the second phase, we propose three operations, i.e., substitution, deletion, and fusion, to optimise S so that (17)-(21) can be simultaneously satisfied.

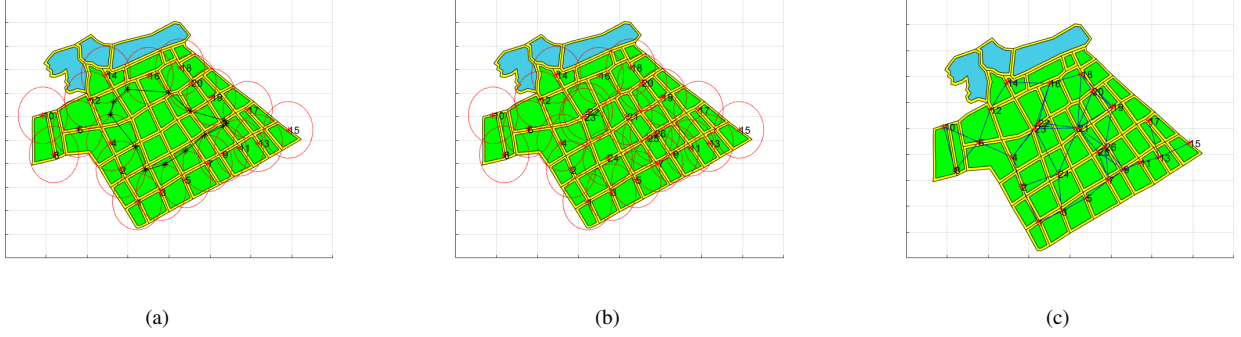


Fig. 11. An diagram of deployment results: (a) The deployment for covering the first layer in which SIL Nodes 1-20 are used to cover the boundary of the first layer. The black star represents the EAI, and the sub-bounded area formed by these black stars is the second layer. (b) The deployment for covering the entire farmland in which SIL Nodes 21-26 are used to cover the vertices (EAIs) of the second layer. (c) The original network topology without optimization.

Algorithm 3 Substitution Operation

Input: S, W

Output: S, W

```

1: for  $s \in S$  do
2:   for  $l \in L \setminus S \cup s$  do
3:     Generate a new solution  $S^*$ , i.e.,  $S^* \leftarrow l \cup S \setminus s$ 
4:     if The new solution  $S^*$  meets coverage requirement, i.e.,  $C_{cov}^{A_f}(S^*) == 1$  then
5:       if The new solution  $S^*$  meets connectivity requirement, i.e.,  $\forall u, v \in [1, |S^*|], m_{uv} \neq 0$  then
6:         Calculate the total weight  $W^*$ , i.e.,  $W^* = \sum_{i \in S^*} w_i$ ;
7:         if  $W^* \geq W$  then
8:            $l^* \leftarrow l$ ;  $W \leftarrow W^*$ ;
9:         end if
10:      end if
11:    end if
12:  end for
13:  Update solution  $S$ , i.e.,  $S \leftarrow l^* \cup S \setminus s$ ;
14: end for
15: Return  $S, W$ ;
  
```

1) *Substitution*: This operation generates a new solution by replacing a substitutable SIL node in S with a new candidate location in $L \setminus S$, so as to maximize the total weight without violating the full coverage and connectivity requirements. The pseudocode of this operation is described in Algorithm 3.

A SIL node $s \in S$ can be substituted by a candidate location l , only if

$$l = \arg \max_{l^* \in (L' \cap L'')} \sum_{i \in (l^* \cup S^*)} w_i \quad (29)$$

s.t.

$$\forall l' \in L', C_{cov}^{A_f}(S') = 1 \quad (30)$$

$$\begin{aligned} & \forall l'' \in L'', \forall u, v \in [1, |S''|], m_{uv} \in M, \\ & M = G(S'') + G(S'')^2 + \dots + G(S'')^{|S''|-1} \quad (31) \\ & m_{uv} \neq 0 \end{aligned}$$

where $S^* = S \setminus s$, $S' = S^* \cup l'$, $S'' = S^* \cup l''$ and $(L', L'') \subset L \setminus S$.

Algorithm 4 Deletion Operation

Input: S

Output: S

```

1: for  $s \in S$  do
2:   Generate a new solution  $S^*$ , i.e.,  $S^* \leftarrow S \setminus s$ 
3:   if The new solution  $S^*$  meets coverage requirement, i.e.,  $C_{cov}^{A_f}(S^*) == 1$  then
4:     if The new solution  $S^*$  meets connectivity requirement, i.e.,  $\forall u, v \in [1, |S^*|], m_{uv} \neq 0$  then
5:       Update solution  $S$ , i.e.,  $S \leftarrow S^*$ ;
6:     end if
7:   end if
8: end for
9: Return  $S$ ;
  
```

2) *Deletion*: This operation is to remove the redundant SIL nodes without violating the full connectivity requirement, so as to reduce the deployment cost. The pseudocode of this operation is described in Algorithm 4.

A redundant SIL node s can be deleted from S , only if

$$\begin{aligned} & \forall u, v \in [1, |S^*|], m_{uv} \in M, \\ & M = G(S^*) + G(S^*)^2 + \dots + G(S^*)^{|S^*|-1} \quad (32) \\ & m_{uv} \neq 0 \end{aligned}$$

where $S^* = S \setminus s$.

3) *Fusion*: This operation is to merge two SIL nodes into a new SIL node, for reducing the deployment cost and maximising the total weight while meeting the full coverage and connectivity requirements. If the merge is successful, a success flag is returned and the new SIL node is reflected in S . Physically, two SIL nodes are removed from S , and a new SIL node is added to S . Otherwise, a failure flag is returned and S is keep the same. The pseudocode of this operation is described in Algorithm 5.

Let (i, j) be a pair of SIL nodes and $d(i, j) \leq 2R$, the fusion is to find a candidate location l to satisfy

$$l = \arg \max_{l^* \in (L' \cap L'')} \sum_{i \in (l^* \cup S')} w_i \quad (33)$$

s.t.

$$\forall l' \in L', C_{cov}^{A_f}(S' \cup l') = 1 \quad (34)$$

Algorithm 5 Fusion Operation

Input: S, R **Output:** S, W

```

1: for  $i, j \in S, i \neq j, d(i, j) \leq 2R$  do
2:    $S' \leftarrow S \setminus \{i, j\}; W \leftarrow 0; Flag \leftarrow 0;$ 
3:   for  $l \in L \setminus S$  do
4:     Generate a new solution  $S^*$ , i.e.,  $S^* \leftarrow S' \cup l;$ 
5:     if The new solution  $S^*$  meets coverage requirement, i.e.,  $C_{cov}^{A_f}(S^*) == 1$  then
6:       if The new solution  $S^*$  meets connectivity requirement, i.e.,  $\forall u, v \in [1, |S^*|], m_{uv} \neq 0$  then
7:         Calculate the total weight  $W^*$ , i.e.,  $W^* = \sum_{i \in S^*} w_i;$ 
8:         if  $W^* \geq W$  then
9:            $S'' \leftarrow S^*; W \leftarrow W^*; Flag \leftarrow 1;$ 
10:        end if
11:       end if
12:     end if
13:   end for
14:   if  $Flag == 1$  then
15:     Update solution  $S$ , i.e.,  $S \leftarrow S'';$ 
16:   end if
17: end for
18: Return  $S, W;$ 

```

TABLE III
SIMULATION PARAMETERS

Parameter	Value	Parameter	Value
P	0(dbm)	$\frac{m}{\text{Map 1/2}}$	800/600(m)
ζ	1(m)	$\frac{n}{\text{Map 1/2}}$	550/450(m)
p_{size}	30	$\frac{A_A}{\text{Map 1/2}}$	15.6/13.6(hm ²)
ρ	4×10^{-3}	$\frac{\alpha}{(A_C/A_G)}$	3.85/3.66

$$\begin{aligned}
 &\forall l'' \in L'', \forall u, v \in [1, |S''|], m_{uv} \in M, \\
 &M = G(S'') + G(S'')^2 + \dots + G(S'')^{|S''|-1} \quad (35) \\
 &m_{uv} \neq 0
 \end{aligned}$$

where $S' = S \setminus \{i, j\}$, $S'' = S' \cup l''$, and $(L', L'') \subset L \setminus S$.

V. SIMULATION

In this section, we carry out simulations to evaluate the performance of our proposed method LDMGA for the wSILD. Specifically, we compare the LDMGA with the Candidate Location Based Greedy Algorithm (CLBGA) [25], the greedy approximate algorithm (GGA) [23], and the randomized greedy algorithm (R-Gr) [28]. CLBGA and R-Gr are designed to solve the grid-based node deployment problem, whose main idea is that the grid point with the maximum coverage ratio is selected to deploy the node in each iteration. These two methods are the same in the deployment strategy, but different in initial solution of the first node. In R-Gr, CLBGA is repeated p_{size} times with different initial solutions, and the best among p_{size}

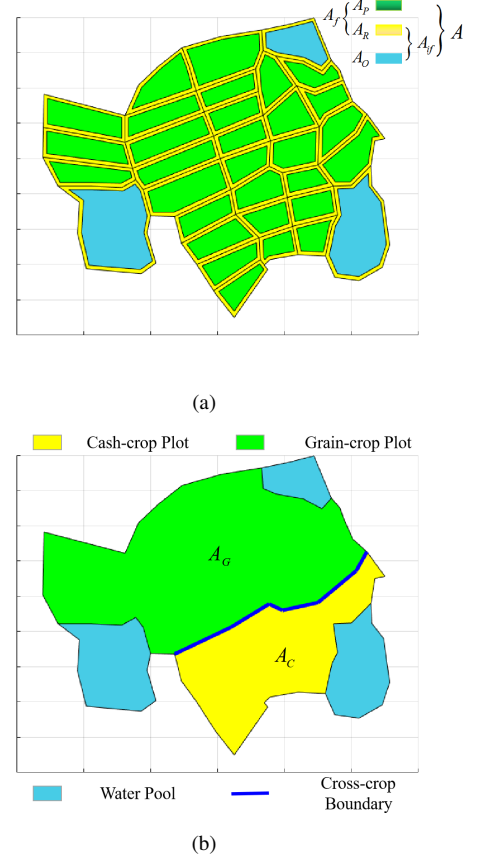


Fig. 12. Map 2: (a) the diagram, (b) the distribution of grain-crop plot and cash-crop plot.

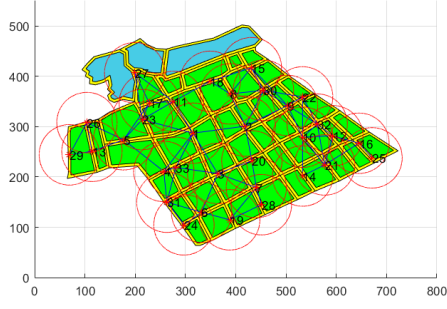
solutions is selected. GAA aims to find the minimum number of nodes in a given set to achieve full coverage. The basic idea is to add the node that can cover an AI with the maximum coverage ratio in each iteration until the full coverage state is achieved.

A. Simulation Setup

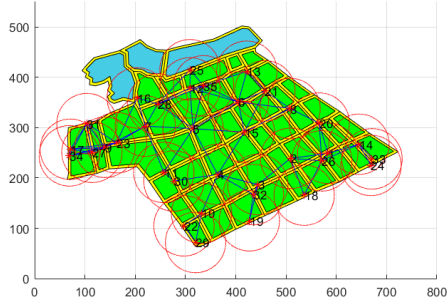
To test the robustness of our proposed LDMGA, in addition to the map presented in Fig. 2, another map given in Fig. 12 is adopted in the simulations. The simulation parameters are listed in Table III. Moreover, to evaluate the efficiency and effectiveness of the proposed method, three experiments are conducted in this section as below:

- 1) To vary the weight coefficient ω , while fixing the effective killing distance $R = 60$ metres and the receiver sensitivity threshold $\gamma_{th} = 4 \times 10^{-8}$.
- 2) To vary the effective killing distance R , while fixing the weight coefficient $\omega = 0.65$ and the receiver sensitivity threshold $\gamma_{th} = 4 \times 10^{-8}$.
- 3) To vary the receiver sensitivity threshold γ_{th} , while fixing the weight coefficient $\omega = 0.65$ and the effective killing distance $R = 60$ metres.

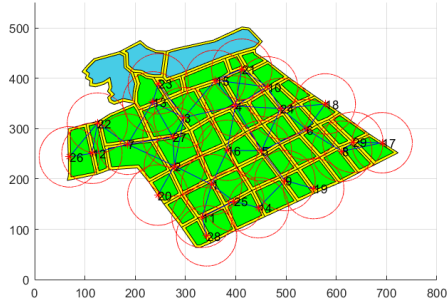
It is worth noting that these simulations are performed by MATLAB R2018b on a PC with 64-bit Microsoft Windows 10 operating system, 8GB RAM and 2.2 GHz-Core i7 CPU. All experimental values are achieved by over 30 independent



(a)



(b)

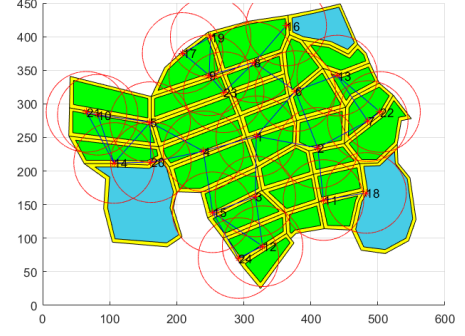


(c)

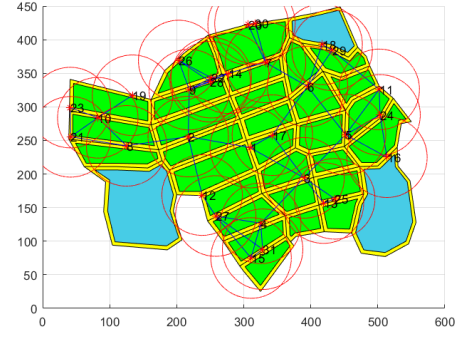


(d)

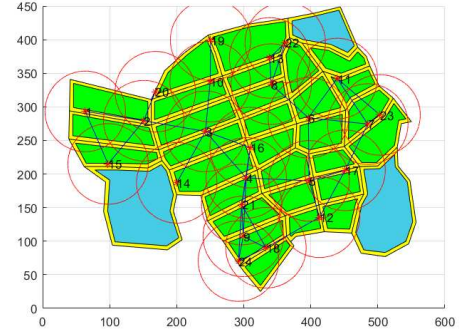
Fig. 13. Deployment of SIL nodes for Map 1 in Fig. 4, with $\omega = 0.65$, $R = 60$ metres and $\gamma_{th} = 4 \times 10^{-8}$. The red star represents the location of a SIL node, the red circle represents the effective killing distance of a SIL node, and the blue line represents the communication link between a pair of SIL nodes: (a) SIL node deployment by GAA, (b) SIL node deployment by CLBGA, (c) SIL node deployment by R-Gr, (d) SIL node deployment by our LDMGA.



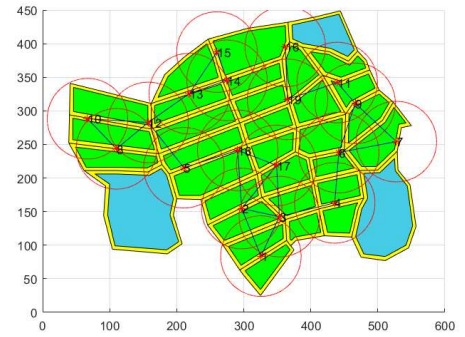
(a)



(b)



(c)



(d)

Fig. 14. Deployment of SIL nodes for Map 2 in Fig. 11, with $\omega = 0.65$, $R = 60$ metres and $\gamma_{th} = 4 \times 10^{-8}$. The red star represents the location of a SIL node, the red circle represents the effective killing distance of a SIL node, and the blue line represents the communication link between a pair of SIL nodes: (a) SIL node deployment by GAA, (b) SIL node deployment by CLBGA, (c) SIL node deployment by R-Gr, (d) SIL node deployment by our LDMGA.

TABLE IV
RESULTS WITH DIFFERENT ω .

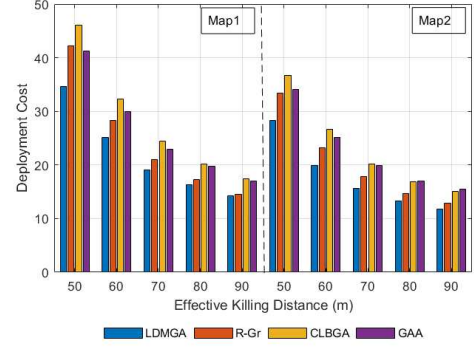
ω	Methods	Map 1		Map 2	
		W	$ S $	W	$ S $
0.55	LDMGA	10.66	25.03	7.53	20.03
	R-Gr	11.23	28.27	8.49	23.2
	CLBGA	12.78	32.3	9.56	26.7
	GAA	11.81	29.97	8.83	25.2
0.65	LDMGA	10.2	25.03	6.9	20.03
	R-Gr	10.67	28.27	7.8	23.2
	CLBGA	12.18	32.3	8.79	26.7
	GAA	11.27	29.97	8.11	25.2
0.75	LDMGA	9.73	25.03	6.27	20.03
	R-Gr	10.11	28.27	7.12	23.2
	CLBGA	11.58	32.3	8.02	26.7
	GAA	10.74	29.97	7.4	25.2
0.85	LDMGA	9.27	25.03	5.64	20.03
	R-Gr	9.55	28.27	6.43	23.2
	CLBGA	10.98	32.3	7.24	26.7
	GAA	10.21	29.97	6.68	25.2
0.95	LDMGA	8.8	25.03	5.01	20.03
	R-Gr	8.98	28.27	5.75	23.2
	CLBGA	10.38	32.3	6.47	26.7
	GAA	9.67	29.97	5.96	25.2

simulations, and for each simulation, a set of candidate locations L are randomly generated according to a uniform random distribution. Additionally, the p_{size} initial solutions of R-Gr are randomly selected from L .

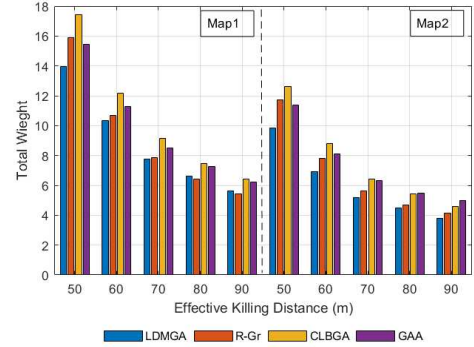
B. Simulation Results

Table IV compares the total weight W and the deployment cost $|S|$ of four deployment methods for various weight coefficient ω . It can be observed that the total weight decreases with the increase in the weight coefficient for these deployment methods. The main reason is that the weight of each candidate location in grain-crop plot decreases with the increase in the weight coefficient, and the increase in the total weight of candidate locations in cash-crop plot cannot compensate the decrease in the total weight of candidate locations in grain-crop plot. Moreover, we also notice that the weight coefficient has no impact on deployment cost. This is indeed justified, since the weight coefficient is only related to the weight of each candidate location, which can be used to fine-tune the location of each SIL node toward the cash-crop plot, but cannot be used to determine the number of SIL nodes. Additionally, our LDMGA dramatically outperforms other deployment methods in terms of deployment cost for both maps.

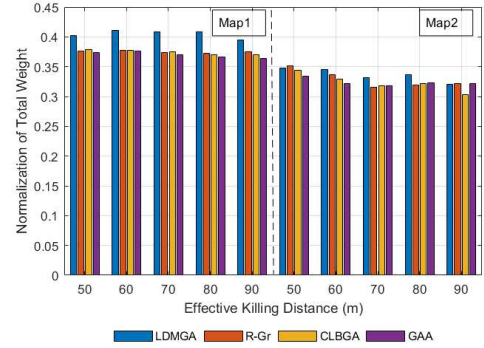
Since the weight coefficient has no effect on deployment cost, we provide deployment examples of GAA, CLBGA, R-Gr, and our LDMGA to illustrate the impact of deployment strategy on deployment cost, which will further illustrate the locations of SIL nodes and the network connectivity. Fig. 13 and 14 plot the SIL node deployment with $\omega = 0.65$, $R = 60$ metres and $\gamma_{th} = 4 \times 10^{-8}$ for these four deployment methods in Map 1 and Map 2. The main parameters are listed in Table V. Note that, to facilitate the comparison on W , the



(a)



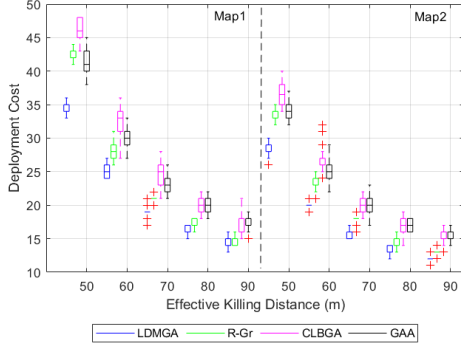
(b)



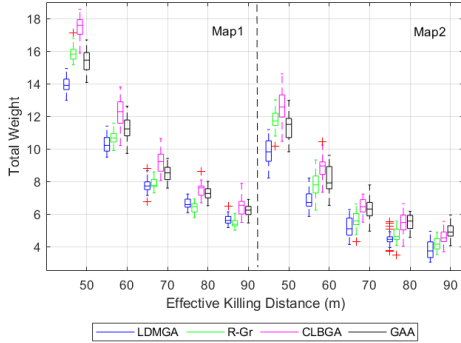
(c)

Fig. 15. Comparison of (a) deployment cost, (b) total weight, and (c) NoW , for four deployment methods with different R .

Normalization of Weight, denoted by NoW , is used, which represents the ratio of total weight to deployment cost. It can be observed that the deployment cost of our LDMGA is obviously less than that of the other methods, mainly because our method deploys SIL nodes round by round from the boundary to the centre of the farmland until the whole area is covered. With the aid of this deployment strategy, the impact of irregular boundary, especially for the boundary with more convex points, on deployment cost can be significantly reduced. Moreover, the design optimization, e.g., deletion and fusion, can further reduce deployment cost.



(a)



(b)

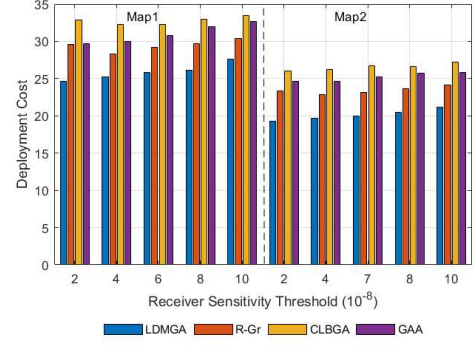
Fig. 16. Boxplots of (a) deployment cost and (b) total weight, for four deployment methods with different R .

TABLE V
MAIN PARAMETERS IN FIGS. 13 AND 14.

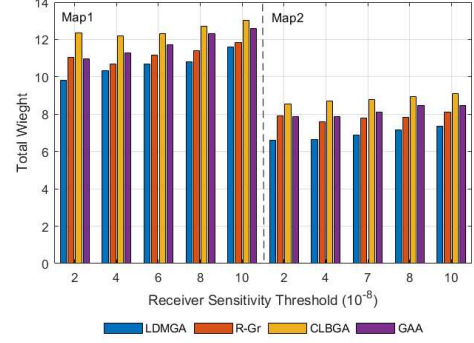
Methods	Map 1			Map 2		
	W	$ S $	NoW	W	$ S $	NoW
LDMGA	9.84	24	0.41	7.146	19	0.376
R-Gr	10.93	29	0.37	8.883	24	0.37
CLBGA	12.96	35	0.37	10.4	31	0.335
GAA	12.61	33	0.382	8.13	24	0.339

Fig. 15 plots the simulation results of deployment cost, total weight and NoW for four deployment methods in Map 1 and Map 2, with R increasing from 50 to 90 by a step 10. The results of 30 independent simulations for deployment cost and total weight with different R are shown in Fig. 16. It can be observed that the deployment cost and total weight decreases with the increase in the effective killing distance, and our LDMGA significantly outperforms the others in terms of deployment cost for both maps. For the total weight, LDMGA has better performance than the other three peer methods in terms of NoW . The CLBGA has the best performance in terms of total weight in most cases, which however needs higher deployment cost.

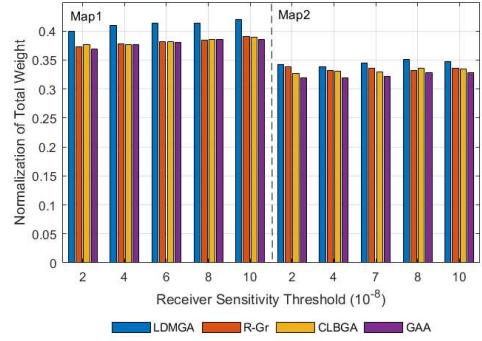
Fig. 17 plots the simulation results of deployment cost, total weight and NoW for four deployment methods in



(a)



(b)



(c)

Fig. 17. Comparison of (a) deployment cost, (b) total weight, and (c) NoW , for four deployment methods with different γ_{th} .

Map 1 and Map 2, with γ_{th} increasing from 2×10^{-8} to 10^{-7} by a step 2×10^{-8} . The results of 30 independent simulations for deployment cost and total weight with different γ_{th} are shown in Fig. 18. It can be seen that in contrary to Experiment 2), the deployment cost and total weight both increases with the increase in the receiver sensitivity threshold. The reason is that the maximum transmission distance of SIL node decreases with the increase in the receiver sensitivity threshold. Therefore, on the premise of ensuring full coverage, all deployment methods need more SIL nodes to guarantee the network connectivity. We also notice that our LDMGA

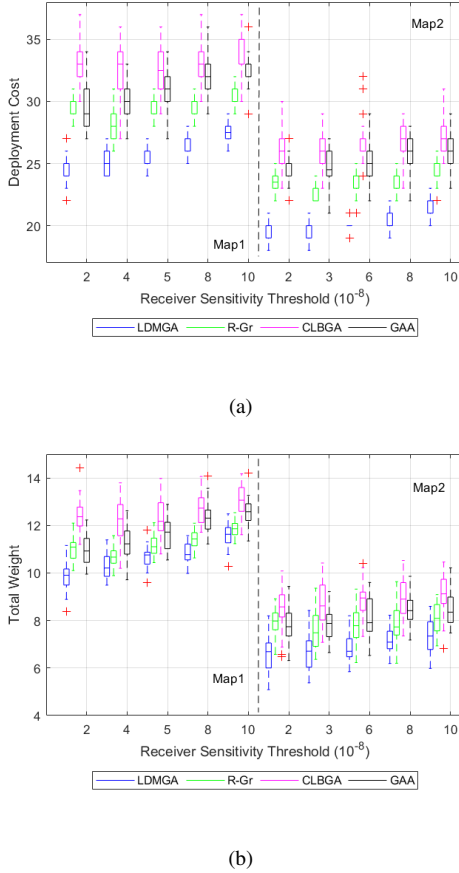


Fig. 18. Boxplots of (a) deployment cost and (b) total weight, for four deployment methods with different γ_{th} .

can guarantee both full coverage and connectivity with the minimum deployment cost for both maps, compared with the other deployment methods. Additionally, the LDMGA obviously outperforms the others in terms of NoW in all the cases.

VI. CONCLUSION

A. Conclusion

Since taking the minimisation of deployment cost as the only optimization objective is not enough to characterise actual agricultural applications, we have further investigated the wSILDP, based on our previous work with the SILDP, in the scenario where the locations of SIL nodes are restricted to a set of weighted candidates on ridges. We have formulated the wSILDP as the WSC problem and proven that it is NP-hard. Because the irregular boundary of farmland seriously impact on the dimension of solution vector for complete coverage, we have proposed a two-phase algorithm, LDMGA, to solve the wSILDP, inspired by the annual rings. In the first phase, SIL nodes are deployed layer by layer from the boundary to the centre until the entire farmland is completely covered. In the second phase, we have fine-tuned these nodes toward the optimal locations to meet the full coverage and connectivity requirements, via three design operations. Simulation results verified that our proposed method achieves better performance

in deployment cost and total weight than the other three peer algorithms.

B. Future Work

For the future work, we plan to further conduct research in the following two aspects:

- 1) Since the disk model is adopted in this paper, we assume that the transmission range of SIL node is regular. However, the irregular transmission range will lead to the existence of asymmetric link, thus the proposed method cannot solve this problem in this case. Therefore, we plan to further study the wSILDP with the irregular transmission range. Additionally, how to use the minimum number of SIL nodes to achieve k -connectivity in the case of irregular transmission range is another work in the future.
- 2) Due to the non-static agricultural environment, the SIL nodes have the same problems as other IoT-related devices, such as node faults. If there is a damaged SIL node, the network built by the proposed method may not be able to connect. Therefore, how to design a deployment mechanism that can provide fault tolerance and maximize the total weight without violating the full coverage and connectivity requirements is another work in the future as well.

REFERENCES

- [1] G. Hu, "Pest automatic counting and publishing system based on pest-killing lamp's voltage disturbance signals," Master's thesis, Nanjing Agricultural University, 2017.
- [2] K. Li, L. Shu, K. Huang, Y. Sun, F. Yang, Y. Zhang, Z. Huo, Y. Wang, X. Wang, Q. Lu, and Y. Zhang, "Research and prospect of solar insecticidal lamps internet of things," *Smart Agriculture*, vol. 1, no. 3, pp. 13–28, 2019. (In Chinese with English abstract).
- [3] D. S. Deif and Y. Gadallah, "Classification of wireless sensor networks deployment techniques," *IEEE Communications Surveys & Tutorials*, vol. 16, no. 2, pp. 834–855, 2014.
- [4] M. Farsi, M. A. Elhosseini, M. Badawy, H. Arafat Ali, and H. Zain Eldin, "Deployment techniques in wireless sensor networks, coverage and connectivity: A survey," *IEEE Access*, vol. 7, pp. 28940–28954, 2019.
- [5] C. Tsai, P. Tsai, J. Pan, and H. Chao, "Metaheuristics for the deployment problem of WSN: A review," *Microprocessors & Microsystems*, vol. 39, no. 8, pp. 1305–1317, 2015.
- [6] W. Bang, "Coverage problems in sensor networks: A survey," *ACM Computing Surveys*, vol. 43, no. 4, pp. 1–56, 2011.
- [7] A. Tripathi, H. P. Gupta, T. Dutta, R. Mishra, K. K. Shukla, and S. Jit, "Coverage and connectivity in wsns: A survey, research issues and challenges," *IEEE Access*, vol. 6, pp. 26971–26992, 2018.
- [8] C. Chang, C. Chang, Y. Chen, and H. Chang, "Obstacle-resistant deployment algorithms for wireless sensor networks," *IEEE Transactions on Vehicular Technology*, vol. 58, no. 6, pp. 2925–2941, 2009.
- [9] B. Wang, H. Xu, W. Liu, and L. T. Yang, "The optimal node placement for long belt coverage in wireless networks," *IEEE Transactions on Computers*, vol. 64, no. 2, pp. 587–592, 2015.
- [10] B. Wang, H. Xu, W. Liu, and H. Liang, "A novel node placement for long belt coverage in wireless networks," *IEEE Transactions on Computers*, vol. 62, no. 12, pp. 2341–2353, 2013.
- [11] C. Bhattacharyya and S. Bhattacharya, "Ldm (layered deployment model): A novel framework to deploy sensors in an irregular terrain," *Wireless Sensor Network*, vol. 3, pp. 189–197, Jan 2011.
- [12] Z. Liao, J. Wang, S. Zhang, and X. Zhang, "A deterministic sensor placement scheme for full coverage and connectivity without boundary effect in wireless sensor networks," *Ad-Hoc and Sensor Wireless Networks*, vol. 19, pp. 327–351, 2013.

- [13] I. Khoufi, P. Minet, A. Laouiti, and E. Livolant, "A simple method for the deployment of wireless sensors to ensure full coverage of an irregular area with obstacles," in *Proceedings of the 17th ACM International Conference on Modeling, Analysis and Simulation of Wireless and Mobile Systems*, pp. 203–210, 2014.
- [14] F. Yang, L. Shu, K. Huang, K. Li, G. Han, and Y. Liu, "A partition-based node deployment strategy in solar insecticidal lamps internet of things," *IEEE Internet of Things Journal*, vol. 7, no. 11, pp. 11223–11237, 2020.
- [15] L. Dai, B. Wang, L. T. Yang, X. Deng, and L. Yi, "A nature-inspired node deployment strategy for connected confident information coverage in industrial internet of things," *IEEE Internet of Things Journal*, vol. 6, no. 6, pp. 9217–9225, 2019.
- [16] H. Wu and M. Shahidehpour, "Applications of wireless sensor networks for area coverage in microgrids," *IEEE Transactions on Smart Grid*, vol. 9, no. 3, pp. 1590–1598, 2018.
- [17] Y. Yoon and Y. Kim, "An efficient genetic algorithm for maximum coverage deployment in wireless sensor networks," *IEEE Transactions on Cybernetics*, vol. 43, no. 5, pp. 1473–1483, 2013.
- [18] Z. Wang, H. Xie, D. He, and S. Chan, "Wireless sensor network deployment optimization based on two flower pollination algorithms," *IEEE Access*, vol. 7, pp. 180590–180608, 2019.
- [19] J. Seok, J. Lee, W. Kim, and J. Lee, "A bipopulation-based evolutionary algorithm for solving full area coverage problems," *IEEE Sensors Journal*, vol. 13, no. 12, pp. 4796–4807, 2013.
- [20] O. M. Alia and A. Al-Ajouri, "Maximizing wireless sensor network coverage with minimum cost using harmony search algorithm," *IEEE Sensors Journal*, vol. 17, no. 3, pp. 882–896, 2017.
- [21] C. Yang and K. Chin, "On nodes placement in energy harvesting wireless sensor networks for coverage and connectivity," *IEEE Transactions on Industrial Informatics*, vol. 13, no. 1, pp. 27–36, 2017.
- [22] A. Khelil and R. Beghdad, *Distributed Algorithm for Coverage and Connectivity in Wireless Sensor Networks*, p. 442C453. IFIP Advances in Information and Communication Technology, 2015.
- [23] Q. Tang, X. Wang, G. Tong, and X. Li, "Studying on minimal cover set node deployment in wireless sensor networks," in *2015 World Symposium on Computer Networks and Information Security (WSCNIS)*, pp. 1–7, 2015.
- [24] H. Mostafaei and M. S. Obaidat, "A greedy overlap-based algorithm for partial coverage of heterogeneous wsns," in *GLOBECOM 2017 - 2017 IEEE Global Communications Conference*, pp. 1–6, 2017.
- [25] J. Zhu and B. Wang, "Sensor placement algorithms for confident information coverage in wireless sensor networks," in *2014 23rd International Conference on Computer Communication and Networks (ICCCN)*, pp. 1–7, 2014.
- [26] M. Rebai, M. L. Berre, H. Snoussi, F. Hnaïen, and L. Khoukhi, "Sensor deployment optimization methods to achieve both coverage and connectivity in wireless sensor networks," *Computers & Operations Research*, vol. 59, pp. 11–21, 2015.
- [27] L. Dai and B. Wang, "Sensor placement based on delaunay triangulation for complete confident information coverage in an area with obstacles," in *2015 IEEE 34th International Performance Computing and Communications Conference (IPCCC)*, pp. 1–8, 2015.
- [28] T. Grossman and A. Wool, "Computational experience with approximation algorithms for the set covering problem," *European Journal of Operational Research*, vol. 101, no. 1, pp. 81–92, 1997.
- [29] K. Lu and H. Sun, "Greedy approximation algorithm of minimum cover set in wireless sensor networks," *Journal of Software*, vol. 21, no. 10, pp. 2656–2665, 2010. (In Chinese with English abstract).
- [30] J. Jiang, L. Fang, H. Zhang, and W. Dou, "An algorithm for minimal connected cover set problem in wireless sensor networks," *Journal of Software*, vol. 17, no. 17, pp. 175–184, 2006. (In Chinese with English abstract).
- [31] M. Younis, S. Lee, I. F. Senturk, and K. Akkaya, *Topology Management Techniques for Tolerating Node Failure*, pp. 273–311. Berlin, Heidelberg: Springer Berlin Heidelberg, 2014.
- [32] J. L. Bredin, E. D. Demaine, M. T. Hajiaghayi, and D. Rus, "Deploying sensor networks with guaranteed fault tolerance," *IEEE/ACM Transactions on Networking*, vol. 18, no. 1, pp. 216–228, 2010.
- [33] "Multi-objective k-connected deployment and power assignment in wsns using a problem-specific constrained evolutionary algorithm based on decomposition," *Computer Communications*, vol. 34, no. 1, pp. 83–98, 2011.
- [34] Lei Gao and J. Nelson, "An algorithm for k-connectivity topology in heterogeneous wireless sensor networks," in *IET Irish Signals and Systems Conference (ISSC 2010)*, pp. 71–75, 2010.
- [35] H. M. Almasaeid and A. E. Kamal, "On the minimum k-connectivity repair in wireless sensor networks," in *2009 IEEE International Conference on Communications*, pp. 1–5, 2009.
- [36] X. Bai, C. Zhang, D. Xuan, and W. Jia, "Full-coverage and k-connectivity (k=14,6) three dimensional networks," in *IEEE INFOCOM 2009*, pp. 388–396, 2009.
- [37] N. Liu, W. Cao, Y. Zhu, J. Zhang, F. Pang, and J. Ni, "Node deployment with k-connectivity in sensor networks for crop information full coverage monitoring," *Sensors*, vol. 16, no. 12, 2016.
- [38] Z. Nutov, "Approximating minimum-power k-connectivity," in *Ad-hoc, Mobile and Wireless Networks* (D. Coudert, D. Simplot-Ryl, and I. Stojmenovic, eds.), (Berlin, Heidelberg), pp. 86–93, Springer Berlin Heidelberg, 2008.
- [39] H. M. Jawad, A. M. Jawad, R. Nordin, S. K. Gharghan, N. F. Abdullah, M. Ismail, and M. J. Abu-AlShaer, "Accurate empirical path-loss model based on particle swarm optimization for wireless sensor networks in smart agriculture," *IEEE Sensors Journal*, vol. 20, no. 1, pp. 552–561, 2020.
- [40] S. Li, H. Gao, and J. Jiang, "Impact of antenna height on propagation characteristics of 2.4 ghz wireless channel in wheat fields," *Transactions of the Chinese Society of Agricultural Engineering*, vol. 25, no. s2, 2009. (In Chinese with English abstract).
- [41] S. Li and H. Gao, "Propagation characteristics of 2.4ghz wireless channel in cornfields," in *2011 IEEE 13th International Conference on Communication Technology*, pp. 136–140, 2011.
- [42] J. Li and F. Wang, "Modeling for wireless channel transmission loss characteristics under rapeseed growth big field environment," *Application Research of Computers*, vol. 34, no. 4, 2017. (In Chinese with English abstract).
- [43] Z. Gao, W. Li, Y. Zhu, Y. Tian, F. Pang, W. Cao, and J. Ni, "Wireless Channel Propagation Characteristics and Modeling Research in Rice Field Sensor Networks," *Sensors*, vol. 18, no. 9, 2018.
- [44] X. Jin, X. Tan, J. Liu, and J. Tang, "Application of frequency trembler pest-killing lamp in the major crops," *Guizhou Agricultural Sciences*, vol. 37, no. 2, pp. 53–54, 2009. (In Chinese with English abstract).
- [45] L. Bian, X. Cai, and Z. Chen, "Effects of light-emitting diode light traps with a suction fan on the population dynamics of the tea leafhopper *Empoasca onukii* (hemiptera: Cicadellidae) within the effective distance," *Journal of Plant Protection*, vol. 46, no. 4, pp. 902–909, 2019. (In Chinese with English abstract).
- [46] X. Ji, N. Wan, and J. Jiang, "Ecological parameters and effective distance of insecticidal lights," *Chinese Journal of Applied Entomology*, vol. 48, no. 3, pp. 669–674, 2011. (In Chinese with English abstract).
- [47] C. Feng and L. Liu, "Preliminary study on solar double-wave trapping light in rice field," *China Rice*, vol. 20, no. 6, pp. 62–65, 2014. (In Chinese with English abstract).
- [48] P. He, S. Ying, W. Xin, and T. Li, "Modeling wireless sensor networks radio frequency signal loss in corn environment," *Multimedia Tools & Applications*, vol. 76, no. 19, pp. 19479–19490, 2016.
- [49] Proakis, *Digital Communications 5th Edition*. McGraw Hill, 2007.
- [50] M. K. Simon and M. Alouini, *Digital Communication over Fading Channels 2th Edition*. John Wiley & Sons, 2005.
- [51] A. F. Molisch, *Wireless Communications*. Wiley-IEEE Press, 2005.
- [52] D. L. Ndzi, A. Harun, F. M. Ramli, M. L. Kamarudin, A. Zakaria, A. Y. M. Shakaff, M. N. Jaafar, S. Zhou, and R. S. Farook, "Wireless, sensor network coverage measurement and planning in mixed crop farming," *Computers & Electronics in Agriculture*, vol. 105, pp. 83–94, 2014.
- [53] D. Balachander, T. R. Rao, and G. Mahesh, "Rf propagation investigations in agricultural fields and gardens for wireless sensor communications," in *Information & Communication Technologies (ICT), 2013 IEEE Conference on*, 2013.
- [54] S. Pirzada, *An Introduction to Graph Theory*. Jun 2012.



Fan Yang received the B.S. degree in communication engineering from Nanjing University of Posts and Telecommunications, Nanjing, China, in 2011 and the M.S. degree in computer application technology from Nanjing Agricultural University, Nanjing, China, in 2014. He is currently working toward the Ph.D. degree with the College of Engineering, Nanjing Agricultural University, China. His research interests include performance analysis and protocol design on networks, Wireless Sensor Networks and IoT.



Ye Liu received the M.S. and Ph.D. degrees from Southeast University, Nanjing, China in 2013 and 2018, respectively. He was a visiting scholar at Montana State University, Bozeman, USA from October 2014 to October 2015. He was a visiting PhD student from February 2017 to January 2018 in the Networked Embedded Systems Group at RISE SICS (Swedish Institute of Computer Science). He is currently a researcher with NAU-Lincoln Joint Research Center of Intelligent Engineering, Nanjing Agricultural University. His current research inter-

ests include wireless sensor networks, energy harvesting systems and mobile crowdsensing.



Lei Shu [M07- SM15] received the B.S. degree in computer science from South Central University for Nationalities, China, in 2002, and the M.S. degree in computer engineering from Kyung Hee University, South Korea, in 2005, and the Ph.D. degree from the Digital Enterprise Research Institute, National University of Ireland, Galway, Ireland, in 2010. Until 2012, he was a Specially Assigned Researcher with the Department of Multimedia Engineering, Graduate School of Information Science and Technology, Osaka University, Japan. He is currently a

Distinguished Professor with the Nanjing Agricultural University, China, and a Lincoln Professor with the University of Lincoln, U.K. He is also the Director of the NAU-Lincoln Joint Research Center of Intelligent Engineering. He has published over 400 papers in related conferences, journals, and books in the areas of sensor networks and Internet of Things. His current H-index is 59 and i10-index is 221 in Google Scholar Citation. His current research interests include wireless sensor networks and Internet of Things. He has also served as a TPC member for more than 150 conferences, DCOSS, MASS, ICC, GLOBECOM, ICCCN, WCNC, and ISCC. He has served over 50 various Co-Chair for international conferences/workshops, such as IWCMC, ICC, ISCC, ICNC, Chinacom, especially the Symposium Co-Chair for IWCMC 2012, ICC 2012, the General Co-Chair for Chinacom 2014, Qshine 2015, Collaboratecom 2017, DependSys 2018, and SCI 2019, the TPC Chair for InisCom 2015, NCCA 2015, WICON 2016, NCCA 2016, Chinacom 2017, InisCom 2017, WMNC 2017, and NCCA 2018. He has also served on the Editorial Boards, including the IEEE Transactions on Industrial Informatics, IEEE Communications Magazine, IEEE Network Magazine, IEEE Systems Journal, IEEE ACCESS, IEEE/CCA JAS.



Timothy Gordon received the B.A. and M.A. degrees in mathematics from Cambridge University, Cambridge, U.K., in 1974 and 1975, respectively, and the Ph.D. degree in applied mathematics from the Department of Applied Mathematics and Theoretical Physics, Cambridge University, in 1983. He is currently a full-time professor with the University of Lincoln, United Kingdom. He joined Lincoln in 2014 having spent ten years at the University of Michigan (UM) as Professor of Mechanical Engineering in the College of Engineering, and heading

the Engineering Research Division at UMs Transportation Research Institute. He was formally Ford Professor at Loughborough University and has worked extensively with the automotive industry. His research is based around vehicle dynamics and control, using automation for safe guidance and collision avoidance in road vehicles. His recent research is on driver modelling, safety system evaluation and the control of vehicle dynamics right up to the limits of road surface friction. During 2006-2012, he was Chair of the Automated Highway Systems standing committee at the Transportation Research Board of the National Academies, Washington DC. He has 150 refereed papers published, mostly in the area of automotive control and active safety systems for road vehicles.



Yuli Yang [S'04-M'08-SM'19] received her Ph.D. degree in Communications & Information Systems from Peking University in July 2007. Since Dec 2019, she has been with the University of Lincoln as a Senior Lecturer in Electrical/Electronic Engineering. From Jan 2010 to Dec 2019, she was with King Abdullah University of Science & Technology, Melikşah University, and the University of Chester on various academic positions. Her industry experience includes working as a Research Scientist with Bell Labs Shanghai, from Aug 2007 to Dec 2009,

and an Intern Researcher with Huawei Technologies, from June 2006 to July 2007. Her research interests include modelling, design, analysis and optimization of wireless systems and networks.